Zero–Reflection Absorbing Boundary Conditions in the Frequency–Domain TLM Method and their Application to Planar Circuit Analysis

Damir Pasalic*, Rüdiger Vahldieck, Jan Hesselbarth** and Jens Bornemann***

***University of Victoria, Dept. of ECE, Victoria, V8W 2Y2, Canada**
****Swiss Federal Institute of Technology, Laboratory for Electromagnetic Fields and Microwave Electronics, 8092 Zürich, Switzerland**
e–mail: vah @ ifh.ee.ethz.ch

Abstract

The frequency–domain TLM (FDTLM) method is extended to include absorbing boundary conditions. An easy-to-implement zero-reflection termination (ZRT) is introduced to simulate open space. A comparison between anisotropic perfectly matched layer (PML), frequently used in time-domain field solvers, shows excellent agreement. The ZRT performance in the FDTLM is demonstrated for scattering matrix analysis of radiating structures and non-shielded planar transmission lines including flip-chip transitions.

Introduction

Since its introduction by Jin and Vahldieck [1] in 1992, the frequency-domain TLM (FDTLM) method has been proven a versatile numerical analysis tool for the calculation of planar structures as well as metal and dielectric waveguide discontinuities. In contrast to the time-domain TLM method, scattering parameters can directly be extracted and thus the method is very well suited for CAD of microwave and millimeter wave integrated circuits. So far, however, the method has only been applied to boxed structures (shielded planar circuits, metallic waveguides etc.). Absorbing boundary conditions known from the FDTD method, i.e. [2], were not available. This has somewhat limited the use of the FDTLM method since radiating structures could not be calculated and also the computational domain was always determined by the size of the shielding box which, in turn, was dependent on how close to the transmission line structure the box walls could be placed without affecting the transmission characteristics. Thus the computational domain was always larger than necessary which led to large computer run time and memory space requirements.
To eliminate unnecessary computer resources so that the FDTLM method can be implemented in an optimisation algorithm, we have recently investigated the use of absorbing boundary conditions [3]. It was found that an an-isotropic perfectly matched layer (PML) and the zero-

reflection termination (ZRT) provide virtually the same results. The ZRT, however, was much easier to implement into the FDTLM algorithm and required fewer computer resources than the PML.
In this paper we focus on the ZRT boundary conditions and its implementation into the FDTLM. We then apply the method to microstrip and co-planar waveguide discontinuities and demonstrate that, in general, ZRT works very well for open structures. This is confirmed by the good agreement between measurements and numerical results from other methods.

Theory

The FDTLM method discretizes the computational domain by a mesh of symmetrical condensed nodes [4], each representing a three-dimensional transmission line network with twelve ports. The electromagnetic field inside the computational domain is represented by a set of voltage waves in the discretization mesh. The voltage waves are scattered at the center of the nodes and are then transferred to the port of each cell by introducing a phase shift term that takes into account the material parameters at the location of each cell.

Any particular boundary condition can be implemented in the FDTLM method by inserting the appropriate reflection coefficients at the ports of the end nodes, i.e., the ports of the transmission lines that touch the boundaries as shown in Fig.1 (top and right boundaries). For a perfect electric conductor, the reflection coefficient Γ is set to –1. For a lossy conductor boundary, the reflection coefficient is chosen accordingly, while for a magnetic wall, Γ is set to +1. It is obvious, that these boundary conditions can easily be implemented into an existing FDTLM algorithm. In fact, even interfacing the FDTLM method with lumped elements is straightforward, although not described in this paper.

A concern in time domain methods is the varying angle of oblique incidence on the boundary. Not so in the FDTLM method since propagation takes place along transmission lines parallel to the direction of the unit vectors of the respective co-ordinate system. Boundaries are placed one-half node distance away from the nodes and are perpendicular to the propagation direction on the transmission lines. Thus the incidence at the boundary is always normal. The remaining variable in this simple but efficient approach is the distance of the ZRT from the actual planar circuit. It was found that placing the boundary condition two to four substrate heights away from the circuit is sufficient for most circuits investigated. To find out how to place the boundary conditions we first place them close to the actual transmission line or discontinuity plane. This would give results on the ‘lossy side’ as the ZRT absorbs a substantial fraction of the transmitted power. Additional calculations at a given frequency with increasing circuit-to-boundary distance will lead to converging results, thus determining the minimum computational domain required for a particular problem.

Results

We first validate the ZRT approach by calculating several microstrip and coplanar waveguide discontinuities and compare the results with measurements and data obtained from other numerical methods.

Fig. 2 shows an NRD guide and its field distribution considering a ZRT wall at two locations: 6.2mm and 1.6mm away from the dielectric–air interface. At both locations the Ey-field appears to be undisturbed by the ZRT wall and follows the analytical data. This indicates very clearly, that the open boundary is well simulated by the ZRT. Next a comparison between results obtained from a FDTLM and a FDTD [6] analysis is shown in Fig. 3 for a simple microstrip lowpass filter example. Also here, very good agreement is obtained in the frequency range of 2 GHz to approximately 17 GHz. In this frequency range, the FDTLM results are even closer than FDTD to the measured data displayed in [6] (not shown here). Some discrepancies are observed above 17 GHz where the FDTD is closer to the measurements. Since our initial runs with this example have been in the operating range of the lowpass filter, i.e. up to appr. 10 GHz, we believe that our discretization mesh was not appropriate to cover the higher-end frequency range of this example.

In order to demonstrate the appropriateness of the ZRT boundary condition even for radiating structures, the frequency dependent input reflection coefficient of an asymmetrically edge-fed rectangular patch antenna [7] is shown in Fig. 4. The absorbing boundaries were placed 4H (substrate thickness H) above the antenna and 8mm from the side of the patch. The results form the FDTLM analysis correctly predicts the general shape of the return loss as illustrated by the almost perfect agreement with measured data taken from [7]. The slight differences between the modelled and measured curve are attributed to some difficulties with the measurement setup and permittivity values as discussed in detail in [7].

We have also tested the ZRT boundaries for the S-parameter analysis of CPW resonators. They represent a greater challenge for the FDTLM simulator than microstrip circuits because of the two field singularities which are extremely close together at the edges of the slots. By placing the boundaries relatively close to the CPW slots, we were able to use more nodes in the areas of field singularities, thus achieving higher accuracy.

First, two CPWs with series stub geometries [8] were analyzed. The first structure (Fig. 5) has straight stubs, whereas the second one (Fig. 6) utilizes L-shaped stubs in order to reduce the radiation loss due to the individual discontinuities. In the simulation of both structures, the ZRT boundaries were placed 3H above and 2H below the CPWs. The side ZRT-wall was placed 2.25 mm from the ends of the stubs. The results of the FDTLM analysis with ZRT boundaries are compared with those obtained from a space-domain integral equation (SDIE) technique [8], and also here excellent agreement is demonstrated (Figs. 5 and 6). In terms of the radiation loss of the two CPW structures, we found that our FDTLM simulation is in very good agreement with the SDIE results of [8], confirming the fact that L-shaped stubs exhibit lower radiation losses than straight ones.

A further example of a CPW resonator, a T-shaped stub structure [9], is illustrated in Fig.7. This time, the finite thickness (3μm) of the metal (gold) was included in the simulation. The thickness of the Al_2O_3 substrate was H=0.254 mm, and a relative permittivity of ε_r=9.9 was assumed. The ZRT boundaries were placed 3H above, 2H below the substrate, and 0.4 mm away from the CPW slots. The FDTLM results are compared with SDIE and experimental data, both obtained from [9], and show good agreement. These successful computations indicate that FDTLM method with ZRT can also be used for the simulation of more complicated uniplanar structures. Finally, Fig.8 illustrates a flip-chip transition between two CPWs. A similar structure was first calculated by Jin and Vahldieck [10] in 1994 considering a shielding box. The structure in Fig.8 was calculated with ZRT boundary conditions (Fig.9) and the results agree well with an FDTD analysis [11].

Conclusions

A very efficient implementation of an open boundary condition into the FDTLM method was presented. The easy to implement zero-reflection termination (ZRT) is tested for S-parameter analysis of radiating and non-radiating planar structures and was found to agree well with measurements and results from other numerical techniques. The use of the ZRT in the FDTLM reduces the computational domain significantly and thus saves memory space and computation time. The introduction of of these absorbing boundaries has extended the scope of the FDTLM method to the analysis of radiation characteristics of planar structures.

References

[1] H. Jin and R. Vahldieck, „The frequency-domain transmission line matrix method —– A new concept," *IEEE Trans. Microwave Theory Tech.*, vol. 40, pp. 2207–2218, Dec. 1992.

[2] J.-P. Berenger, „A perfectly matched layer for the absorption of electromagnetic waves," *J. Comput. Physics*, vol. 114, pp. 185–200, Oct. 1994.

[3] D. Pasalic, R. Vahldieck, and J. Hesselbarth, „The frequency-domain TLM method with absorbing boundary conditions," *IEEE MTT–S Int. Microwave Symp. Dig.*, 1669–1672, June 1999.

[4] P. Johns, „A symmetrical condensed node for the TLM method," *IEEE Trans. Microwave Theory Tech.*, vol. 35, pp. 370–377, Apr. 1987.

[5] R.-C. Hsieh and J.-T. Kuo, „Fast full-wave analysis of planar microstrip circuit elements in stratified media," *IEEE Trans. Microwave Theory Tech.*, vol. 46, pp. 1291–1297, Sep. 1998.

[6] D.M. Sheen, S.A. Ali, M.D. Abou-zahra, and J.A. Kong, „Application of the three-dimensional finite-difference time-domain method to the analysis of planar microstrip circuits," *IEEE Trans. Microwave Theory Tech.*, vol. 38, pp. 849–857, July 1990.

[7] S.-C. Wu, N.G. Alexopoulos, and O. Fordham, „Feeding structure contribution to radiation by patch antennas with rectangular boundaries," *IEEE Trans. Antennas Propagat.*, vol. 40, pp. 1245–1249, Oct. 1992.

[8] N.I. Dib, W.P. Harokopus, Jr., G.E. Ponchak, and L.P.B. Katehi, „A comparative study between shielded and open coplanar waveguide discontinuities," *Int. J. Microwave Millimeter-Wave Computer-Aided Eng.*, vol. 2, no. 4, pp. 331–341, 1992.

[9] K. Hettak, N. Dib, A.-F. Sheta, and S. Toutain, „A class of novel uniplanar series resonators and their implementation in original applications," *IEEE Trans. Microwave Theory Tech.*, vol. 46, pp. 1270–1276, Sept. 1998.

[10] H. Jin, R. Vahldieck and H. Minkus, „FDTLM analysis of flip-chip interconnections," *Proc. 24th Europ. Microwave Conf.*, pp. 1259–1264, 1994.

[11] H.H.M. Ghouz, E.-B. El-Sharawy, „Finite-difference time-domain analy-sis of flip-chip interconnects with staggered bumps," *IEEE Trans. Microwave Theory Tech.*, vol. 44, no. 6, pp. 960–963, June 1996.

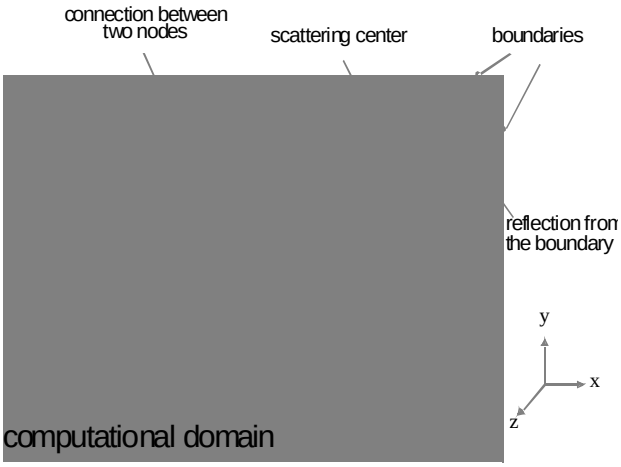

Fig.1 *Discretization mesh with FDTLM nodes.*

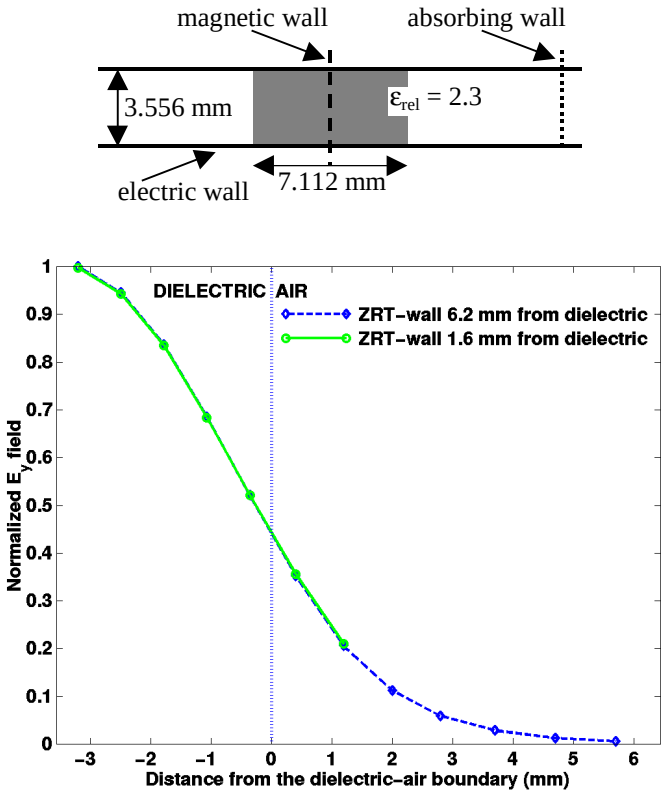

Fig. 2 *Normalized |Ey| field of the LSE_{01} mode in a NRD guide. Absorbing boundary (ZRT) 1.6 mm and 6.2 mm from the dielectric.*

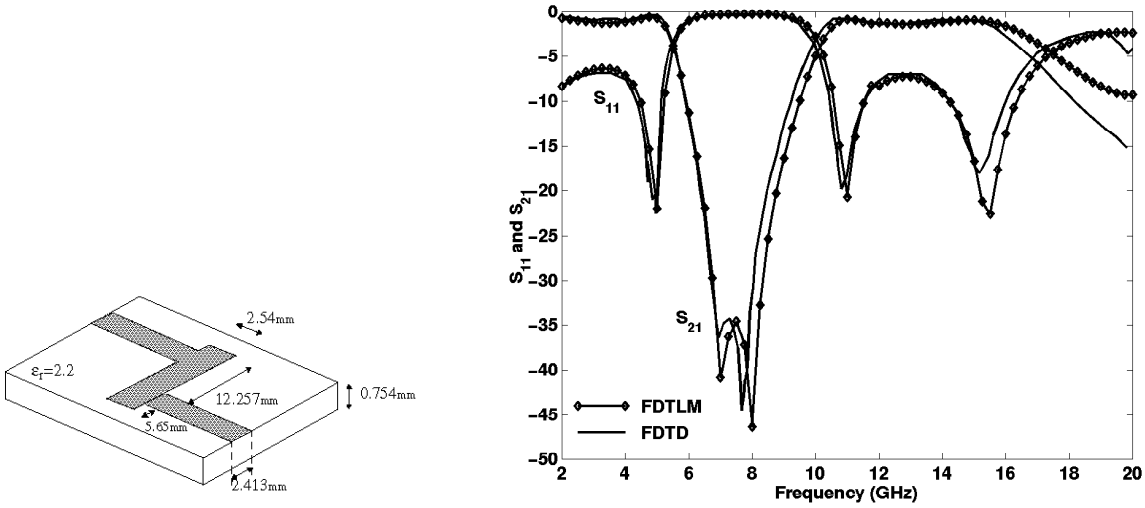

Fig.3 *Comparison between FDTD [6] and FDTLM methods for a microstrip low–pass filter.*

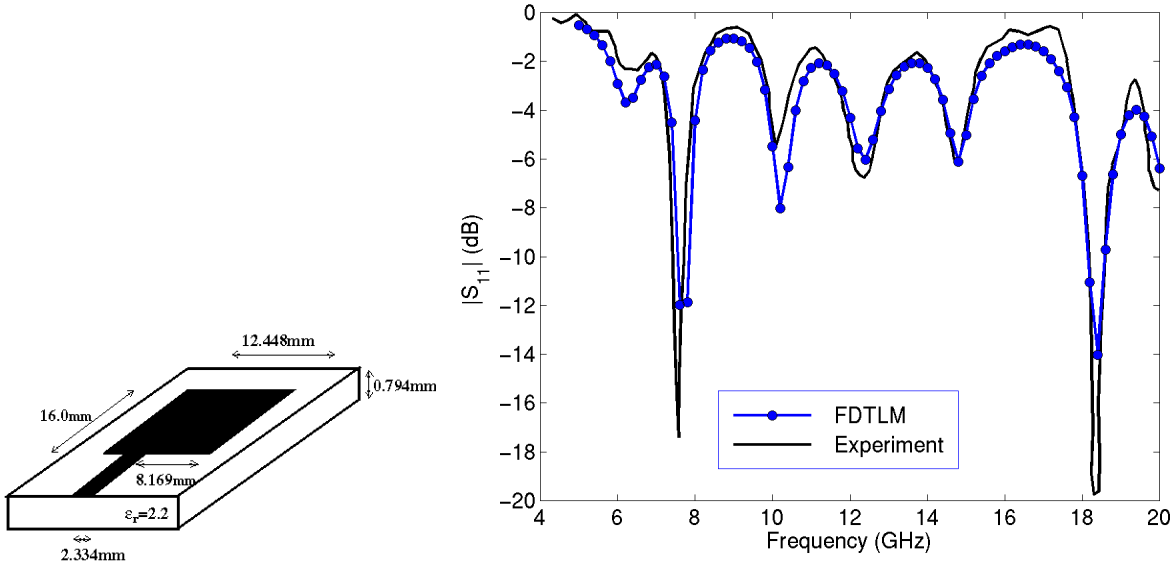

Fig. 4 *Input reflection coefficient of an asymmetrically edge–fed microstrip patch antenna. Design and experimental data according to [7].*

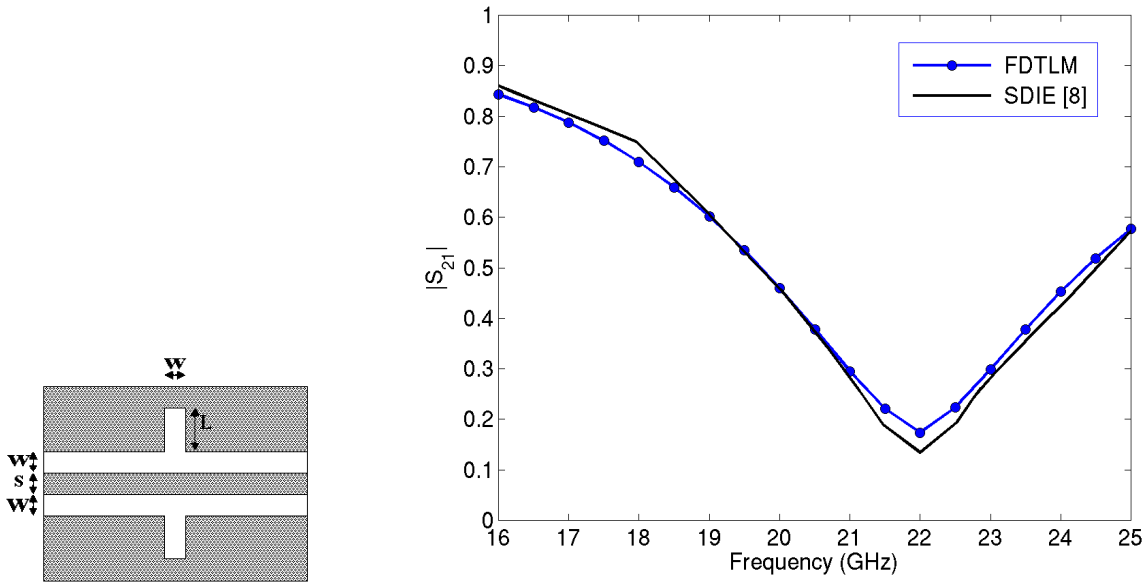

Fig.5 *Transmission coefficient of a CPW with series stubs. w=0.225mm, s=0.45mm, L=1.35mm, substrate thickness H=0.635mm, ε_{rel}=9.9. SDIE data from [8].*

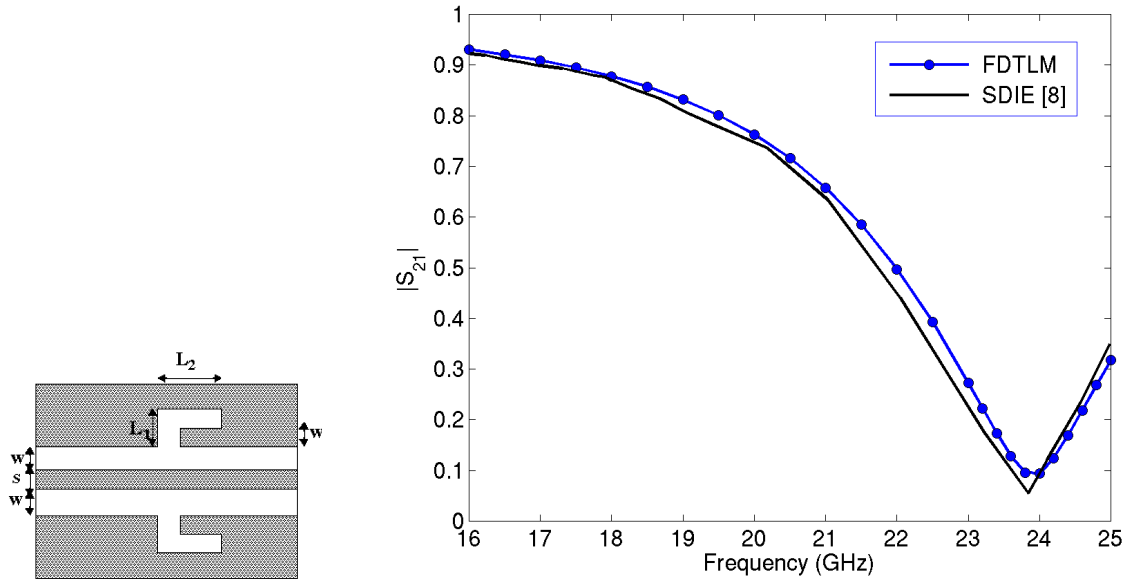

Fig.6 *Transmission coefficient of a CPW with L–shaped series stubs. w=0.225mm, s=0.45mm, L_1=0.45mm, L_2=1.125mm, substrate thickness H=0.635mm, ε_{rel}=9.9. SDIE data from [8].*

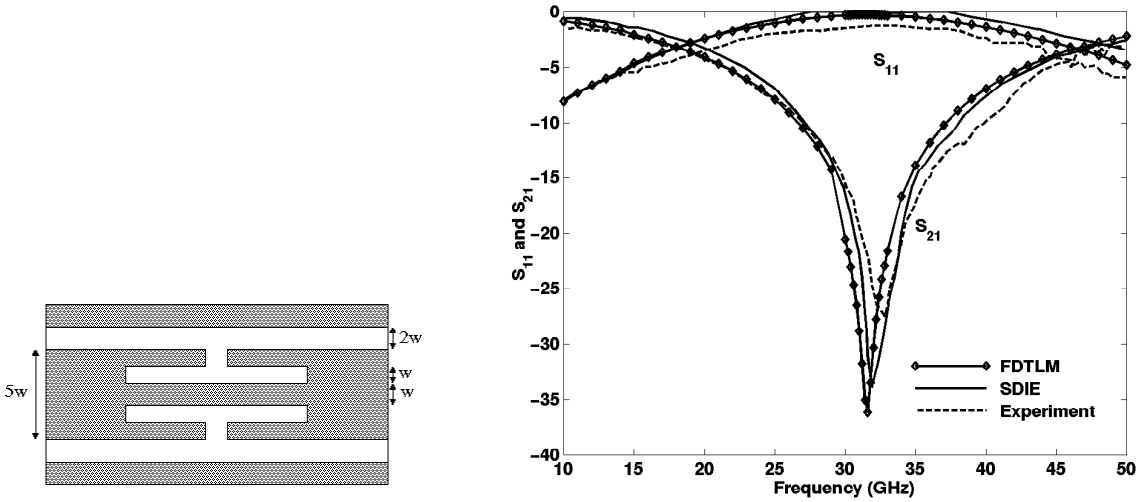

Fig. 7 *S–parameters of T–shaped CPW series stubs. Length=2.025mm, w=0.025mm, substrate thickness H=0.635mm, ε_{rel}=9.9. SDIE and experimental data from [9].*

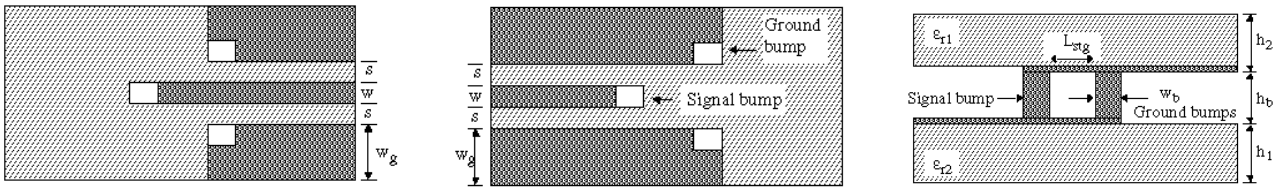

top view of CPW chip *top view of motherboard* *side view*

Fig.8 *Flip–chip structure. h_1=h_2=0.36mm, h_b=w=s=w_b=0.12mm, w_g=0.6mm, ε_{r1}= ε_{r2}=12.9. L_{stg}=0 for the structure with in–line bumps and L_{stg}=2s for the structure with staggered bumps.*

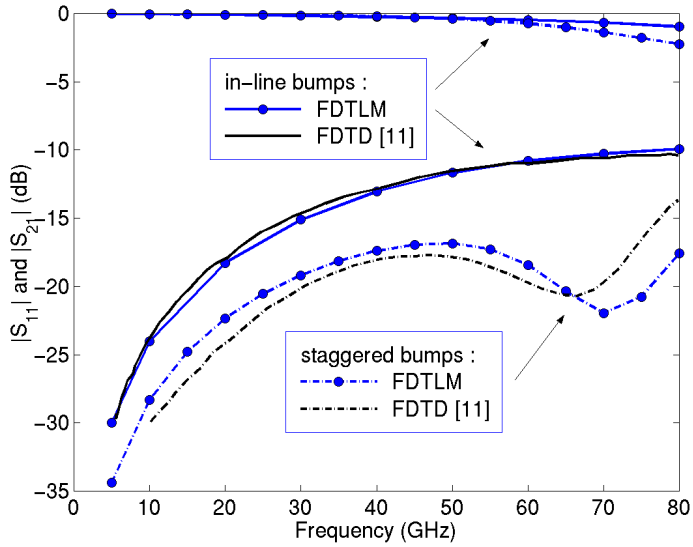

Fig.9 *S–parameters of the flip–chip transition shown in Fig. 8. FDTD data from [11].*